

π and σ mesons at finite temperature and density in the NJL model with dimensional regularization

T. Inagaki

Information Media Center, Hiroshima University, Higashi-Hiroshima, Japan

D. Kimura

Department of Physical Science, Hiroshima University, Higashi-Hiroshima, Japan

A. Kvinikhidze

A. Razmadze Mathematical Institute of Georgian Academy of Sciences, Tbilisi, Georgia

(Dated: February 6, 2020)

Abstract

Dynamical Symmetry breaking and meson masses are studied in the Nambu-Jona-Lasinio (NJL) model at finite temperature and chemical potential using the dimensional regularization. Since the model is not renormalizable in four space-time dimensions, physical results and parameters depend on the regularization method. Following the imaginary time formalism, we introduce the temperature, T and the chemical potential, μ . The parameters in the model are fixed by calculating the pion mass and decay constant in the dimensional regularization at $T = \mu = 0$.

PACS numbers: 11.10.Kk, 11.30.Qc, 12.39.-x

I. INTRODUCTION

QCD is a fundamental theory of quarks and gluons whose coupling constant is large at low energy scale. Therefore one cannot adopt the perturbative expansion in powers of the coupling constant at low energy. To study physics in a hadronic phase we can not avoid considering the non-perturbative effect of QCD. One of the possible ways to evaluate the phenomena in the hadronic phase is to use a low energy effective theory. Some phenomenological parameters are introduced to construct the low energy effective theory which is simpler than QCD to deal with. NJL model is one of the low energy effective theories of QCD [1], for a review see Refs.[2, 3, 4, 5]. The model has the same chiral symmetry as QCD and the symmetry is broken down dynamically. Thus it is often used to study symmetry properties of QCD in the hadronic phase.

The NJL model contains four-fermion interactions. Since a four-fermion interaction is a dimension six operator, the NJL model is not renormalizable in four space-time dimensions. To obtain finite expressions we must regularize the theory. In such a non-renormalizable model most of the physical quantities depend on the regularization method and a parameter introduced to regularize the theory. For example, a cut-off scale is introduced as a parameter in a cut-off regularization. The coupling constant and the cut-off scale are determined phenomenologically.

The regularization in general may break some of the symmetries of the theory. For example a naive three dimensional cut-off breaks Lorentz and gauge invariance [6]. In the present paper we employ the dimensional regularization. It keeps most of the symmetries of the theory, including the general covariance. We regard the space-time dimensions as one of the parameters in the effective theory. Thus the dimensions should be determined in some low energy phenomena which have some relation with chiral symmetry breaking.

There are some works investigating NJL model in the dimensional regularization. The general properties of the renormalization and the renormalization group is studied in arbitrary dimensions $2 < D < 4$ [7, 8, 9]. In Refs.[10, 11, 12, 13, 14, 15, 16] the NJL model is considered as a prototype model of composite Higgs. The phase structure of dynamical symmetry breaking is analyzed at high temperature, density, electro-magnetic field and curvature. But we have no established fundamental theory of composite Higgs models at high energy scale. Thus the physical scale of the theory has not been fixed and the contribution

of the current fermion mass has not been analyzed.

In Ref.[17] the dimensional regularization is modified to keep four dimensional properties of the non-renormalizable theory as much as possible. To achieve this goal the dimensional regularization is applied to only the radial part in loop integrals. It is one of the analytic regularization. The meson contribution to the chiral symmetry breaking is also analyzed in the NJL model with the modified dimensional regularization [18]. The procedure is easily extended to the finite temperature and chemical potential. However, the phenomenologically consistent dimensions are less than two in this approach. Because of the infrared divergence it seems to be difficult to obtain a finite result at finite temperature.

In the present paper we regard the NJL model as a low energy effective theory of QCD and apply the dimensional regularization not only to the radial part but also to the angular parts of internal momenta in loop integrals. We include the effect of the current quark mass and fix the scale through the observed properties of pseudo-scalar mesons, the pion mass and the decay constant at zero density and temperature. The constituent quark mass and the meson properties are evaluated in thermal equilibrium.

The paper is organized in the following way. First we apply the dimensional regularization to the NJL model with two flavors of quarks. As is well-known, the small mass of quarks explicitly breaks the chiral symmetry. Thus the chiral symmetry is only approximate. In such a model we evaluate the phase structure of the theory. We need to perform renormalization as well to define a positive coupling constant. In Sec.II we calculate the mass of scalar and pseudo-scalar mesons. We take the massless quarks limit and show that the dimensional regularization keeps the Nambu-Goldstone modes massless. A relationship between the space-time dimensions and the physical mass scale is also discussed. In Sec.IV we introduce the thermal effect in the imaginary time formalism and evaluate the effective potential. In Sec.V we calculate the mass of scalar and pseudo-scalar mesons at finite T and μ . The three massless poles of pseudo-scalar mesons survive at higher temperature and chemical potential. At the end concluding remarks are given.

II. DYNAMICAL SYMMETRY BREAKING

The chiral symmetry is broken when the composite operator of a quark and an anti-quark, $\bar{\psi}\psi$, develops a non-vanishing expectation value. It is caused by the QCD dynamics and is

called dynamical symmetry breaking.

The NJL model is one of the simplest models of dynamical chiral symmetry breaking. The model is originally introduced to evaluate the low energy properties of hadrons as a bound state of some primary fermion fields [1]. The Lagrangian of the two-flavor NJL model is defined by

$$\mathcal{L} = \bar{\psi}(i\not{\partial} - m)\psi + g_\pi^0 \{(\bar{\psi}\psi)^2 + (\bar{\psi}i\gamma_5\tau^a\psi)^2\} , \quad (1)$$

where g_π^0 is an effective coupling constant, τ^a represents the isospin Pauli matrices, and $m = \text{diag}(m_u, m_d)$ is the mass matrix of up and down quarks. In the Lagrangian (1) we omit the color and the flavor index.

In the limit of massless quarks this Lagrangian is invariant under the global flavor transformation

$$\psi \rightarrow e^{i\theta^a\tau^a}\psi, \quad (2)$$

and the chiral transformation

$$\psi \rightarrow e^{i\theta^a\tau^a\gamma^5}\psi. \quad (3)$$

The quark mass term violates these symmetries explicitly. When the composite operator $\bar{\psi}\psi$ develops a non-vanishing expectation value, the quark acquires a mass and the chiral symmetry is broken dynamically.

The vacuum expectation value of the composite operator $\bar{\psi}\psi$ can be found by solving the gap equation. The gap equation of the NJL model in D dimensions is

$$\langle\sigma\rangle = 2ig_\pi^0 \int \frac{d^Dk}{(2\pi)^D} \text{tr} S(k), \quad (4)$$

where $S(k)$ is the fermion propagator and "tr" denotes trace with respect to flavor, color and spinor indices,

$$S(k) \equiv \frac{1}{\not{k} - m - \langle\sigma\rangle + i\epsilon}. \quad (5)$$

Integration over k takes the gap equation to the form

$$\begin{aligned} \langle\sigma\rangle &= \frac{2N_c g_\pi^0}{(2\pi)^{D/2}} \Gamma\left(1 - \frac{D}{2}\right) \sum_{j \in \{u, d\}} (m_j + \langle\sigma\rangle) [(m_j + \langle\sigma\rangle)^2]^{(D/2-1)} \\ &\equiv g_\pi^0 A(D) \sum_{j \in \{u, d\}} (m_j + \langle\sigma\rangle) [(m_j + \langle\sigma\rangle)^2]^{(D/2-1)}, \end{aligned} \quad (6)$$

where N_c is the number of colors and $A(D)$ is defined by

$$A(D) \equiv \frac{2N_c}{(2\pi)^{D/2}} \Gamma\left(1 - \frac{D}{2}\right). \quad (7)$$

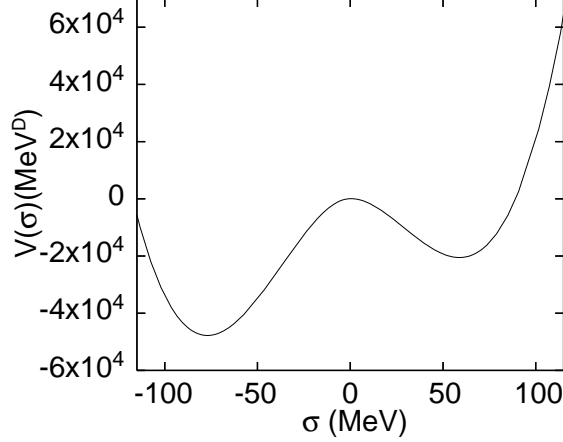


FIG. 1: Typical behaviors of the effective potential ($D = 2.8$, $m_u = 3\text{MeV}$, $m_d = 5\text{MeV}$ and $g_\pi^0 = -0.01\text{MeV}^{2-D}$).

The gap equation (6) has three solutions. To find the stable solution we evaluate the effective potential for the scalar channel, σ , (see, for example Ref.[10])

$$V(\sigma) = \frac{\sigma^2}{4g_\pi^0} - \frac{A(D)}{2D} \sum_{j \in \{u,d\}} [(m_j + \sigma)^2]^{D/2}. \quad (8)$$

Extrema of the effective potential satisfy the gap equation (6). The most stable solution is determined by observing the minimum of the effective potential. As is shown in the Fig.1, we find the minimum at a negative value of σ for a negative coupling constant, g_π^0 , with a finite current quark mass. We note that the expectation value, $\langle \bar{\psi}\psi \rangle \sim -\frac{1}{2g_\pi^0} \langle \sigma \rangle$, has a negative value as usual.

At the massless limit, $m \rightarrow 0$, the gap equation (6) is simplified and the solutions are:

$$\langle \sigma \rangle = 0, \quad (9)$$

$$(\langle \sigma \rangle^2)^{D/2-1} = \frac{1}{2g_\pi^0 A(D)}. \quad (10)$$

The non-vanishing solution (10) is stabler, see Fig.1. It shows that the composite operator $\bar{\psi}\psi$ develops a non-vanishing expectation value and the chiral symmetry is broken dynamically. It should be noted that

$$A(D) < 0, \quad \text{for } 2 < D < 4. \quad (11)$$

The left hand side of the Eq.(10) is real and positive. To find a real solution of Eq.(10) we must set a negative value to the coupling constant g_π^0 . It is one of characteristic features of the dimensional regularization.

A. Renormalization

The Lagrangian (1) is not renormalizable for $D = 4$. However, the renormalization is sometimes useful to connect the results in the different regularization procedure. Here we renormalize parameters in our model.

In the leading order of the $1/N$ expansion the radiative correction of the four-fermion coupling for the scalar channel is given by the summation of all bubble type diagrams,

$$\begin{aligned}
 G_s(p^2, \langle \sigma \rangle) &\equiv \text{diagram 1} + \text{diagram 2} \\
 &+ \text{diagram 3} \\
 &+ \text{diagram 4} \dots \text{diagram 5} \\
 &= 2g_\pi^0 \left(1 + \frac{\Pi_s(p^2)}{2g_\pi^0 - \Pi_s(p^2)} \right) = \frac{4(g_\pi^0)^2}{2g_\pi^0 - \Pi_s(p^2)},
 \end{aligned} \tag{12}$$

where the self-energy $\Pi_s(p^2)$ is

$$\begin{aligned}
 \Pi_s(p^2) &= \text{bubble diagram} = 4i(g_\pi^0)^2 \int \frac{d^D k}{(2\pi)^D} \text{tr}[S(k)S(k-p)] \\
 &= 2(g_\pi^0)^2 (D-1)A(D) \sum_{j \in \{u, d\}} \int_0^1 dx L_j^{D/2-1},
 \end{aligned} \tag{13}$$

with $L_j = (m_j + \langle \sigma \rangle)^2 - x(1-x)p^2$.

We renormalize the coupling constant g_π^0 by imposing the following renormalization condition

$$\begin{aligned}
 G_s(p^2 = 0, \langle \sigma \rangle = M_0) &\equiv Z_g(M_0) G_s^r(p^2 = 0, \langle \sigma \rangle = M_0) \\
 &= \frac{4Z_g(M_0)g_\pi^0}{\sum_{j \in \{u, d\}} [(m_j + M_0)^2]^{D/2-1}} \\
 &= \frac{4g_\pi^r}{\sum_{j \in \{u, d\}} [(m_j + M_0)^2]^{D/2-1}},
 \end{aligned} \tag{14}$$

where we introduce the renormalization constant, $Z_g(M_0)$. The superscript r stands for the renormalized quantities and M_0 is a renormalization scale.

At the limit $p^2 = 0$ the self-energy $\Pi_s(p^2)$ simplifies to

$$\Pi_s(p^2 = 0)|_{\langle\sigma\rangle=M_0} = 2(g_\pi^0)^2(D-1)A(D) \sum_{j \in \{u,d\}} [(m_j + M_0)^2]^{D/2-1}. \quad (15)$$

Thus the renormalization constant is given by

$$Z_g(M_0) = \frac{1}{2} \frac{\sum_{j \in \{u,d\}} [(m_j + M_0)^2]^{D/2-1}}{1 - g_\pi^0(D-1)A(D) \sum_{j \in \{u,d\}} [(m_j + M_0)^2]^{D/2-1}}. \quad (16)$$

Therefore the renormalized coupling g_π^r is found to be

$$\frac{1}{g_\pi^0} \frac{1}{\sum_{j \in \{u,d\}} [(m_j + M_0)^2]^{D/2-1}} = \frac{1}{2g_\pi^r} + (D-1)A(D). \quad (17)$$

We rewrite the gap equation (6) in terms of the renormalized coupling constant g_π^r as

$$\frac{\sum_{j \in \{u,d\}} (m_j + \langle\sigma\rangle)[(m_j + \langle\sigma\rangle)^2]^{D/2-1}}{\sum_{j \in \{u,d\}} [(m_j + M_0)^2]^{D/2-1}} = \langle\sigma\rangle \left(\frac{1}{2g_\pi^r A(D)} + D - 1 \right). \quad (18)$$

In the massless limit $m \rightarrow 0$, the non-trivial solution of the gap equation is given by

$$(\langle\sigma\rangle^2)^{(D/2-1)} = \left(\frac{1}{2g_\pi^r A(D)} + D - 1 \right) (M_0^2)^{(D/2-1)}. \quad (19)$$

A real solution for $\langle\sigma\rangle$ exists for $1/g_\pi^r < 1/g_\pi^{cr}$,

$$g_\pi^{cr} = \frac{1}{2(1-D)A(D)} > 0 \quad \text{for } 2 < D < 4. \quad (20)$$

The critical coupling is real and positive. It should be noted that the broken phase is realized for $g_\pi^r > g_\pi^{cr} > 0$ or $g_\pi^r < 0$.

It may be useful to rewrite the Eqs. (17) and (18) in terms of the critical coupling,

$$\frac{1}{g_\pi^0} \frac{1}{\sum_{j \in \{u,d\}} [(m_j + M_0)^2]^{D/2-1}} = \frac{1}{2g_\pi^r} - \frac{1}{2g_\pi^{cr}}, \quad (21)$$

and

$$\frac{\sum_{j \in \{u,d\}} (m_j + \langle\sigma\rangle)[(m_j + \langle\sigma\rangle)^2]^{1-D/2}}{\sum_{j \in \{u,d\}} [(m_j + M_0)^2]^{1-D/2}} = \frac{2\langle\sigma\rangle}{A(D)} \left(\frac{1}{g_\pi^r} - \frac{1}{g_\pi^{cr}} \right). \quad (22)$$

From Eq.(21) it is clear that the bare coupling g_π^0 should be negative in the broken phase, $1/g_\pi^r < 1/g_\pi^{cr}$, in the dimensional regularization.

The renormalization group β function is defined by [8, 9],

$$\beta(g_\pi^r) \equiv M_0 \left. \frac{\partial g_\pi^r}{\partial M_0} \right|_{g_\pi^0}. \quad (23)$$

Using Eq.(22) in Eq.(23) we obtain

$$\beta(g_\pi^r) = 2(D-2) \frac{M_0 \sum_{j \in \{u,d\}} [(m_j + M_0)^2]^{(D-3)/2}}{\sum_{j \in \{u,d\}} [(m_j + M_0)^2]^{D/2-1}} \frac{g_\pi^r (g_\pi^{cr} - g_\pi^r)}{g_\pi^{cr}}. \quad (24)$$

The ultraviolet stable fixed point appears at the critical coupling, $g_\pi^r = g_\pi^{cr}$.

III. MESON MASSES

To describe a bound state in the hadronic phase non-perturbative effects of QCD should be considered. Here we study meson masses in the NJL model at the leading order of the $1/N$ expansion.

A. Pseudo-scalar mesons

First we calculate the pion mass in the two-flavor NJL model. It corresponds to the Nambu-Goldstone modes at the massless quark limit. Since the current quark mass explicitly breaks the chiral symmetry, the pion mass should be proportional to the current quark mass in the broken phase.

The pion mass is defined by the pole of the propagator for a pseudo-scalar channel. The leading order of the $1/N$ expansion is described by the summation of infinite number of the

bubble diagrams,

$$\begin{aligned}
G_5^{ab}(p^2, \langle \sigma \rangle) &= \pi^a \text{---}\text{X}\text{---} \pi^b + \pi^a \text{---}\text{---}\text{---}\text{---}\text{---}\pi^b \\
&+ \pi^a \text{---}\text{---}\text{---}\text{---}\text{---}\pi^b \\
&+ \pi^a \text{---}\text{---}\text{---}\text{---}\text{---}\pi^b \dots \pi^b \\
&= \frac{4(g_\pi^0)^2}{2g_\pi^0 - \Pi_5^a(p^2)} \delta^{ab} \equiv \frac{Z_\pi^a M_0^{4-D}}{m_{\pi^a}^2 - p^2 + O(p^4)} \delta^{ab},
\end{aligned} \tag{25}$$

where we insert the renormalization scale $M_0^{D/2-2}$ to impose the correct mass dimensions on Z_π . $\Pi_5^a(p^2)$ is the self-energy for the pseudo-scalar channel which is given by

$$\begin{aligned}
\Pi_5^a(p^2) &= i\gamma^5 \tau^a \text{---}\text{---}\text{---}\text{---}\text{---} i\gamma^5 \tau^a \\
&= 4i(g_\pi^0)^2 \int \frac{d^D k}{(2\pi)^D} \text{tr}[i\gamma^5 \tau^a S(k) i\gamma^5 \tau^a S(k-p)].
\end{aligned} \tag{26}$$

Integrating over the D -dimensional momentum k , we obtain

$$\begin{aligned}
\Pi_5^{1,2}(p^2) &= 4(g_\pi^0)^2 A(D) \int_0^1 dx \left[(1-D)x(1-x)p^2 + \frac{D}{2}x(m_u + \langle \sigma \rangle)^2 \right. \\
&\quad \left. + \frac{D}{2}(1-x)(m_d + \langle \sigma \rangle)^2 + \left(1 - \frac{D}{2}\right)(m_u + \langle \sigma \rangle)(m_d + \langle \sigma \rangle) \right] \\
&\quad \times [x(m_u + \langle \sigma \rangle)^2 + (1-x)(m_d + \langle \sigma \rangle)^2 - x(1-x)p^2]^{D/2-2},
\end{aligned} \tag{27}$$

and

$$\begin{aligned}
\Pi_5^3(p^2) &= 2(g_\pi^0)^2 A(D) \int_0^1 dx \sum_{j \in \{u,d\}} [(1-D)x(1-x)p^2 + (m_j + \langle \sigma \rangle)^2] \\
&\quad \times [(m_j + \langle \sigma \rangle)^2 - x(1-x)p^2]^{D/2-2}.
\end{aligned} \tag{28}$$

We can analytically calculate the momentum integral at finite p^2 , but it is enough to evaluate the self-energy near $p^2 = 0$ to observe the massless pole of the Nambu-Goldstone

mode. Straightforward calculations lead to

$$\begin{aligned} \Pi_5^{1,2}(p^2 \sim 0) = & 4(g_\pi^0)^2 A(D) \left[\frac{\sum_{j \in \{u,d\}} [(m_j + \langle \sigma \rangle)^2]^{(D-1)/2}}{\sum_{j \in \{u,d\}} [(m_j + \langle \sigma \rangle)^2]^{1/2}} - f(D)p^2 \right] \\ & + O(p^4), \end{aligned} \quad (29)$$

and

$$\begin{aligned} \Pi_5^3(p^2 \sim 0) = & (g_\pi^0)^2 A(D) \left[2 \sum_{j \in \{u,d\}} [(m_j + \langle \sigma \rangle)^2]^{D/2-1} \right. \\ & \left. + \left(1 - \frac{D}{2}\right) p^2 \sum_{j \in \{u,d\}} [(m_j + \langle \sigma \rangle)^2]^{D/2-2} \right] + O(p^4), \end{aligned} \quad (30)$$

where $f(D)$ is given by

$$\begin{aligned} f(D) = & \frac{1}{[(m_d + \langle \sigma \rangle)^2 - (m_u + \langle \sigma \rangle)^2]^3} \\ & \times \left\{ \left(\frac{2}{D} - 1 \right) [(m_d + \langle \sigma \rangle)^{D+2} - (m_u + \langle \sigma \rangle)^{D+2}] \right. \\ & + \left(\frac{2}{D} + 1 \right) [(m_d + \langle \sigma \rangle)^D (m_u + \langle \sigma \rangle)^2 - (m_d + \langle \sigma \rangle)^2 (m_u + \langle \sigma \rangle)^D] \\ & - \left(\frac{4}{D} - 1 \right) [(m_d + \langle \sigma \rangle)^{D+1} (m_u + \langle \sigma \rangle) - (m_d + \langle \sigma \rangle) (m_u + \langle \sigma \rangle)^{D+1}] \\ & \left. - (m_d + \langle \sigma \rangle)^{D-1} (m_u + \langle \sigma \rangle)^3 + (m_d + \langle \sigma \rangle)^{D-1} (m_u + \langle \sigma \rangle)^3 \right\}. \end{aligned} \quad (31)$$

In the isospin symmetric case, $m_u = m_d$, $\Pi_5^{1,2}(p^2 \sim 0)$ coincides with $\Pi_5^3(p^2 \sim 0)$.

Further we obtain the the pion wave function renormalization constants,

$$Z_{\pi^{1,2}}^{-1} = -A(D)f(D)M_0^{4-D}, \quad (32)$$

and

$$Z_{\pi^3}^{-1} = \frac{A(D)}{4} \left(1 - \frac{D}{2}\right) M_0^{4-D} \sum_{j \in \{u,d\}} [(m_j + \langle \sigma \rangle)^2]^{D/2-2}. \quad (33)$$

Neglecting $O(p^4)$ terms, the pion masses are found to be

$$Z_{\pi^{1,2}}^{-1} M_0^{D-4} m_{\pi^{1,2}}^2 = \frac{1}{2g_\pi^0} - A(D) \frac{(\langle \sigma \rangle + m_u)^{D-1} + (\langle \sigma \rangle + m_d)^{D-1}}{2\langle \sigma \rangle + m_u + m_d}, \quad (34)$$

and

$$Z_{\pi^3}^{-1} M_0^{D-4} m_{\pi^3}^2 = \frac{1}{2g_\pi^0} - \frac{1}{2} A(D) \sum_{j \in \{u,d\}} [(m_j + \langle \sigma \rangle)^2]^{D/2-1}. \quad (35)$$

In the massless quark limit Eqs.(34) and (35) read

$$Z_\pi^{-1} M_0^{D-4} m_\pi^2 \rightarrow \frac{1}{2g_\pi^0} - A(D)(\langle\sigma\rangle^2)^{D/2-1}. \quad (36)$$

Substituting the non-trivial solution of the gap equation (10) into Eq.(36), we observe that the pion mass disappears. Therefore the pion propagator has massless pole and thus the Nambu-Goldstone mode remains in the dimensional regularization. This is natural given the fact that dimensional regularization does not damage Ward-Takahashi identity, whereas cut-off regularization does [6]. If the constituent quark mass is not generated, the above expression is rewritten as

$$Z_\pi^{-1} M_0^{D-4} m_\pi^2 \rightarrow \frac{1}{2g_\pi^0} = \left(\frac{1}{2g_\pi^r} - \frac{1}{2g_\pi^{cr}} \right) (M_0^2)^{D/2-1}. \quad (37)$$

Since the renormalization constant Z_π is positive definite, the pion mass squared is negative in the broken phase, $1/g_\pi^r < 1/g_\pi^{cr}$. Such a tachyon pole is compensated by the constituent quark mass. On the other hand inverse of the renormalization constant Z_π^{-1} is divergent and a massless pion pole appears in the symmetric phase, $1/g_\pi^r > 1/g_\pi^{cr}$.

B. The scalar meson

Next we calculate the meson mass in the scalar channel. The propagator for the scalar channel in the leading order of the $1/N$ expansion is given in Eq.(12)

$$G_s(p^2, \langle\sigma\rangle) = \frac{4(g_\pi^0)^2}{2g_\pi^0 - \Pi_s(p^2)}. \quad (38)$$

The scalar meson mass (given that the corresponding pole is not located on the real axis) is obtained by observing the extremum for $|G_s(p^2 = m_\sigma^2, \langle\sigma\rangle)|$. We can find the corresponding pole for $D \gtrsim 2.2$. It can not be found for $D \lesssim 2.2$ and for soft mode in the next section. The extremum condition Eq. (38) for scalar meson mass is applicable for more general cases.

First we discuss the massless pole in the scalar channel. It is not realistic but useful to understand the symmetry properties of NJL model. If the scalar meson is light enough, we can employ the same procedure as in the previous subsection. Thus we use the definition for m_σ similar to m_π .

$$G_s(p^2, \langle\sigma\rangle) \equiv \frac{Z_\sigma M_0^{4-D}}{m_\sigma^2 - p^2 + O(p^4)}. \quad (39)$$

The self-energy $\Pi_s(p^2)$ defined in Eq.(13) is expanded near $p^2 \sim 0$ as

$$\begin{aligned} \Pi_s(p^2 \sim 0) = & 2(g_\pi^0)^2(D-1)A(D) \left[\sum_{j \in \{u,d\}} [(m_j + \langle \sigma \rangle)^2]^{D/2-1} \right. \\ & \left. + \frac{1}{6} \left(1 - \frac{D}{2}\right) p^2 \sum_{j \in \{u,d\}} [(m_j + \langle \sigma \rangle)^2]^{D/2-2} \right] + O(p^4). \end{aligned} \quad (40)$$

Thus the renormalization constant for the scalar wave function is obtained by

$$Z_\sigma^{-1} = \frac{D-1}{12} \left(1 - \frac{D}{2}\right) A(D) M_0^{4-D} \sum_{j \in \{u,d\}} [(m_j + \langle \sigma \rangle)^2]^{D/2-2}. \quad (41)$$

It has a positive definite value for $2 < D < 4$. In the present approximation the scalar mass is given by

$$Z_\sigma^{-1} M_0^{D-4} m_\sigma^2 = \frac{1}{2g_\pi^0} - \frac{1}{2} A(D)(D-1) \sum_{j \in \{u,d\}} [(m_j + \langle \sigma \rangle)^2]^{D/2-1}. \quad (42)$$

In the massless quark limit it becomes

$$Z_\sigma^{-1} M_0^{D-4} m_\sigma^2 \rightarrow \frac{1}{2g_\pi^0} (2-D) = \left(\frac{1}{2g_\pi^r} - \frac{1}{2g_\pi^{cr}} \right) (2-D) (M_0^2)^{D/2-1}. \quad (43)$$

where we used the gap equation (10). As is shown in Sec.II, the bare coupling g_π^0 is always negative in the broken phase for $2 < D < 4$. Thus the sigma mass squared is real and positive for $1/g_\pi^r > 1/g_\pi^{cr}$. As the inverse of the coupling $1/g_\pi^r$ increases the sigma mass decreases. For $1/g_\pi^r \geq 1/g_\pi^{cr}$ the renormalization constant Z_σ vanishes. Hence a massless pole appears for the scalar channel. The sigma meson degenerates with the pion in the symmetric phase.

If we do not consider the constituent quark mass, the sigma meson mass degenerates with the pion mass (37) in the limit of massless quarks. The tachyon pole (37) shows that the vacuum is unstable and the constituent quark mass should be generated.

Since the scalar meson is heavy in the real world, we do not apply the expression (42) to evaluate the real scalar meson mass. Furthermore, there is no pole for $p^2 \leq 4(\langle \sigma \rangle + m)^2$. An imaginary part appears in the self-energy for $p^2 > 4(\langle \sigma \rangle + m)^2$. The imaginary part corresponds to the decay width of the sigma meson. To find the sigma meson resonance we numerically calculate the pole of the propagator.

C. Dimensions and physical scale

In this subsection we discuss the physical scale and coupling constant in term of the space-time dimensions. Since the NJL model is phenomenological model of QCD, the scale of the model should be determined to reproduce the observable physical quantities. Here we calculate the pion decay constant and the pion mass as typical quantities in the hadronic phase. To consider the QCD interaction we set $N_c = 3$. In the present model the space-time dimensions D in the loop integrals is also regarded as one of the parameters of the phenomenological model.

Inserting the measured values $m_\pi^0 = 135.0\text{MeV}$ and $m_\pi^\pm = 139.6\text{MeV}$ into Eqs.(34) and (35), we can obtain the matching condition for the coupling constant g_π and the space-time dimensions D with the physical scale. But the main part of the mass difference between the neutral and the charged pion arise from the electro-magnetic interaction which is not considered here [19]. Thus we inspect only the isospin symmetric limit $m_\pi^0 = m_\pi^\pm \simeq 136\text{MeV}$ and set $m_u = m_d$ below.

We start with the relationship in the current algebra (See, for example, appendix in Ref. [20].) The pion decay constant f_π is written as

$$f_\pi = -Z_\pi^{-1/2} \langle \sigma \rangle. \quad (44)$$

From the Gell-Mann-Oakes-Renner relation [23] we obtain

$$f_\pi^2 m_\pi^2 = \frac{\langle \sigma \rangle}{4g_\pi^0} M_0^{4-D} (m_u + m_d). \quad (45)$$

The constituent quark mass $\langle \sigma \rangle$ is determined by the gap equation (6). Substituting the measured values $m_\pi = 136\text{MeV}$, $f_\pi = 93\text{MeV}$ and the solution of the gap equation we obtain the matching condition for the coupling constant g_π , the space-time dimensions D and the renormalization scale M_0 with the physical scale. After some numerical calculations we get the physical scale for g_π and M_0 as a function of the space-time dimensions D .

In Fig.2 the curves satisfy the relations (44) and (45) on $D - g_\pi^0$ and $D - M_0$ plane for $m_u = m_d = 3, 4$ and 5MeV . As is shown in Fig. 2, the bare coupling constant and the renormalization scale has no strong dependence on the current quark mass. The renormalization scale is found to be below the pion mass. In Fig.3 we illustrate the behaviors of the constituent quark mass and the expectation value of the composite operator of a quark and

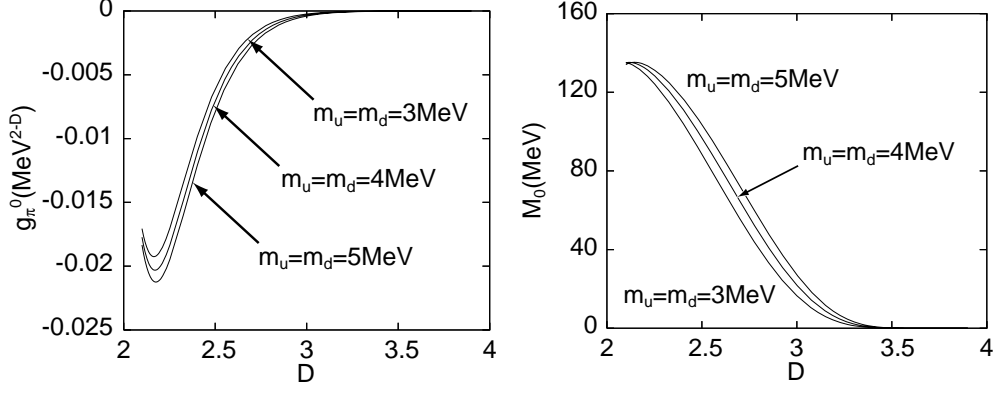


FIG. 2: The physical scale for the bare coupling constant g_π^0 and the renormalization scale M_0 are shown as a function of the space-time dimensions D for $N_c = 3$, $m_u = m_d = 3, 4$ and 5MeV .

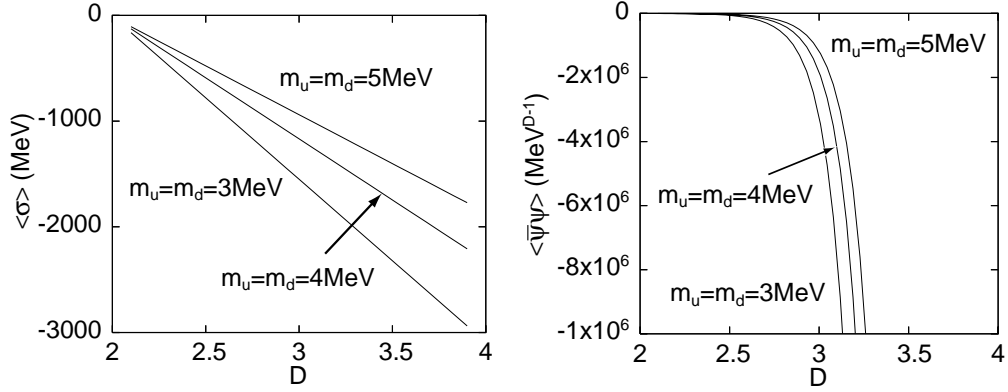
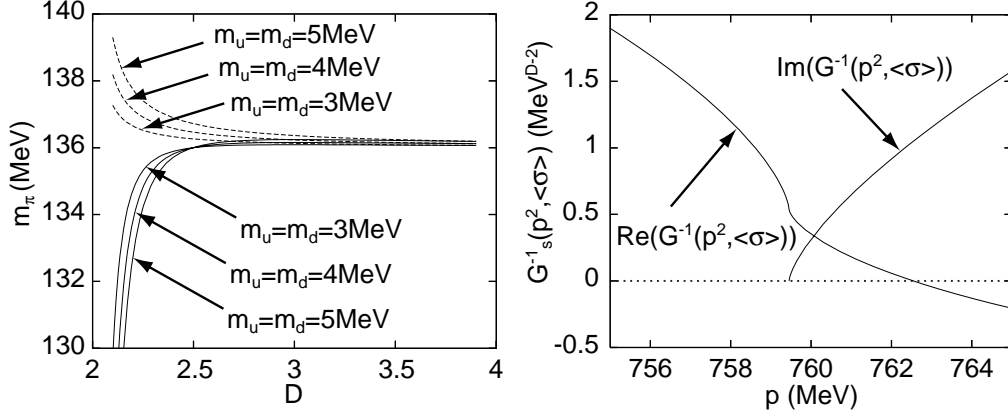


FIG. 3: The constituent quark mass $\langle\sigma\rangle$ and the expectation value $\langle\bar{\psi}\psi\rangle$ are shown as a function of the space-time dimensions D .

an anti-quark, $\langle\bar{\psi}\psi\rangle \sim -\frac{1}{2g_\pi^0}\langle\sigma\rangle$, for the parameters fixed by (44) and (45). To obtain the constituent quark mass near 300MeV we should consider the lower space-time dimensions or larger current quark mass. The expectation value $\langle\bar{\psi}\psi\rangle$ has strong dependence on the space-time dimensions. But the normalized value, $\langle\bar{\psi}\psi\rangle M_0^{4-D}$, varies less than 0.1% between two and four dimensions and found to be

$$\langle\bar{u}u\rangle M_0^{4-D} \simeq \begin{cases} -(298.7\text{MeV})^3 & (m_u = m_d = 3\text{MeV}), \\ -(271.4\text{MeV})^3 & (m_u = m_d = 4\text{MeV}), \\ -(252.0\text{MeV})^3 & (m_u = m_d = 5\text{MeV}). \end{cases} \quad (46)$$

Inserting the non-trivial solution of the gap equation into Eq.(35) and taking $m_u = m_d =$



(a) Pion mass from Eq.(35) (dashed lines) and Eq.(48) (full lines). (b) $G_s^{-1}(p^2, \langle\sigma\rangle)$ for $D = 2.4$ and $m_u = m_d = 5$ MeV.

FIG. 4: Solutions for Eq.(48) and Eq.(49).

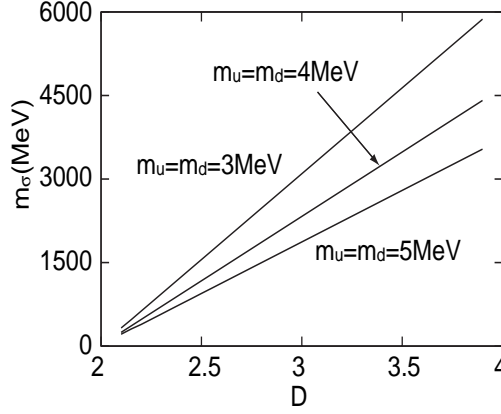


FIG. 5: Sigma meson mass from Eq. (49).

m we get

$$Z_\pi^{-1} M_0^{D-4} m_\pi^2 \simeq \frac{m}{2g_\pi^0 \langle\sigma\rangle} + \mathcal{O}\left(\left(\frac{m}{\langle\sigma\rangle}\right)^2\right). \quad (47)$$

The Gell-Mann-Oakes-Renner relation (45) is reproduced from Eqs.(44) and (47). Thus the Eq. (35) should be consistent with the model independent relationships (44) and (45).

In Figs.4 and 5 [38] we calculate the pion and the sigma meson mass by numerically solving the equations

$$G_5^{-1}(p^2 = m_\pi^2, \langle\sigma\rangle) = \frac{1}{2g_\pi^0} - \frac{1}{4(g_\pi^0)^2} \Pi_5(p^2 = m_\pi^2) = 0, \quad (48)$$

and

$$\frac{\partial}{\partial p}|G_s(p^2 = m_\sigma^2, \langle\sigma\rangle)| = 0, \quad (49)$$

with the gap equation. As is clearly seen in Fig. 4 (a), the results for m_π are found at the physical pion mass scale $\simeq 136\text{MeV}$ for $D \gtrsim 2.2$. The approximation in Eq. (35) seems to be valid for higher dimensions. A typical behaviors of the real and the imaginary part of $G_s^{-1}(p^2, \langle\sigma\rangle)$ is shown in Fig. 4 (b). The sigma meson develops the heavier mass for higher dimensions in Fig.5. The sigma meson width is given by the imaginary part of G_s^{-1} . In the leading order of $1/N$ expansion, it is found to be an unrealistic value, $O(1)$ MeV. As is pointed out in Ref [21], a higher order correction, $\pi\pi$ scattering, is essential for the sigma width. To discuss the sigma meson width one should calculate the next to leading order correction in $1/N$ expansion.

IV. DYNAMICAL SYMMETRY BREAKING AT FINITE T AND μ

To define the thermal equilibrium the time direction has to be fixed. This breaks general covariance however, it is important not to introduce an additional violation of the covariance through the regularization. Thus we apply the dimensional regularization to the NJL model in the thermal equilibrium and extend the above analysis to the finite temperature T and the chemical potential μ .

First we discuss the phase structure of the theory. It is expected that the broken chiral symmetry is restored at high temperature and/or large chemical potential. Following the standard procedure of the imaginary-time formalism, we introduce the temperature and the chemical potential to the NJL model in D dimensions [10]. Hence the gap equation (4) is modified as

$$\langle\sigma\rangle = 2g_\pi^0 \frac{1}{\beta} \sum_n \int \frac{d^{D-1}\mathbf{k}}{(2\pi)^{D-1}} \text{tr} S_{\beta\mu}(k), \quad (50)$$

where $S_{\beta\mu}(k)$ is the fermion propagator at finite T and μ ,

$$S_{\beta\mu}(k) \equiv \frac{1}{\mathbf{k} \cdot \boldsymbol{\gamma} - (\omega_n - i\mu)\gamma_4 + m + \langle\sigma\rangle - i\epsilon}. \quad (51)$$

Due to the anti-periodicity of the fermion field the k^0 integral is replaced by the summation over $\omega_n = (2n+1)\pi/\beta$. We note that the flavor symmetry is broken by the quark mass and the chemical potential in the thermal equilibrium (see, for example, Ref.[22].)

Integrating over the momentum in Eq.(50), we obtain

$$\begin{aligned}\langle\sigma\rangle &= -\sqrt{2}g_\pi^0 A(D-1) \sum_{j \in \{u,d\}} (m_j + \langle\sigma\rangle) \\ &\quad \times \frac{1}{\beta} \sum_n [(\omega_n - i\mu)^2 + (m_j + \langle\sigma\rangle)^2]^{(D-3)/2}.\end{aligned}\quad (52)$$

We also perform the summation in Eq.(50) and get the other expression,

$$\begin{aligned}\langle\sigma\rangle &= g_\pi^0 A(D) \sum_{j \in \{u,d\}} (m_j + \langle\sigma\rangle) [(m_j + \langle\sigma\rangle)^2]^{D/2-1} \\ &\quad - \frac{2\sqrt{2}N_c g_\pi^0}{(2\pi)^{(D-1)/2}} \frac{1}{\Gamma\left(\frac{D-1}{2}\right)} \int_0^\infty k^{D-2} dk \sum_{j \in \{u,d\}} \frac{m_j + \langle\sigma\rangle}{\sqrt{k^2 + (m_j + \langle\sigma\rangle)^2}} \\ &\quad \times \left(\frac{1}{1 + e^{\beta(\sqrt{k^2 + (m_j + \langle\sigma\rangle)^2} + \mu)}} + \frac{1}{1 + e^{\beta(\sqrt{k^2 + (m_j + \langle\sigma\rangle)^2} - \mu)}} \right).\end{aligned}\quad (53)$$

The result exactly reproduces the one obtained in Ref.[10] at the massless quark limit.

At the zero temperature limit the gap equation (53) simplifies to

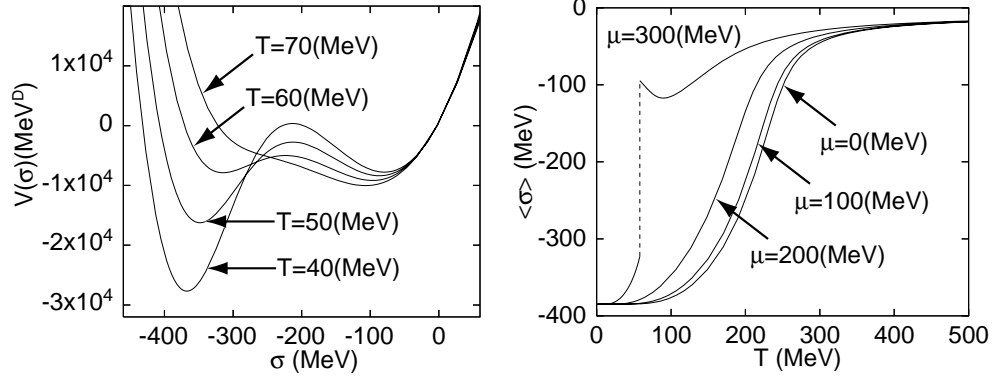
$$\begin{aligned}\langle\sigma\rangle &= g_\pi^0 A(D) \sum_{j \in \{u,d\}} (m_j + \langle\sigma\rangle) [(m_j + \langle\sigma\rangle)^2]^{D/2-1} \\ &\quad - \frac{2\sqrt{2}N_c g_\pi^0}{(2\pi)^{(D-1)/2}} \frac{1}{\Gamma\left(\frac{D-1}{2}\right)} \sum_{j \in \{u,d\}} \int_0^\infty k^{D-2} dk \frac{m_j + \langle\sigma\rangle}{\sqrt{k^2 + (m_j + \langle\sigma\rangle)^2}} \\ &\quad \times \theta(\mu - \sqrt{k^2 + (m_j + \langle\sigma\rangle)^2}).\end{aligned}\quad (54)$$

For $\mu < m_u + \langle\sigma\rangle$ and $\mu < m_d + \langle\sigma\rangle$ the theta function vanishes and we obtain the same solution with zero chemical potential.

$$\langle\sigma\rangle = g_\pi^0 A(D) \sum_{j \in \{u,d\}} (m_j + \langle\sigma\rangle) [(m_j + \langle\sigma\rangle)^2]^{D/2-1}.\quad (55)$$

Hence, the chemical potential does not contribute to the constituent quark mass $\langle\sigma\rangle$ at $T = 0$, $\mu < m_u + \langle\sigma\rangle$ and $\mu < m_d + \langle\sigma\rangle$.

To find the stable solution we evaluate the effective potential $V(\sigma)$ at finite T and μ . It



(a) Behaviors of the effective potential (b) Behaviors of the constituent quark mass $\langle\sigma\rangle$.
at $\mu = 300(\text{MeV})$.

FIG. 6: Typical behaviors of the effective potential and the constituent quark mass at finite T and μ in $D = 2.4$ and $m_u = m_d = 5\text{MeV}$.

is obtained by integrating over σ in the gap equation (53), we get

$$\begin{aligned}
V(\sigma) = & \frac{\sigma^2}{4g_\pi^0} - \frac{A(D)}{2D} \sum_{j \in \{u,d\}} [(m_j + \sigma)^2]^{D/2} \\
& - \frac{1}{\beta} \frac{\sqrt{2}N_c}{(2\pi)^{(D-1)/2}} \frac{1}{\Gamma\left(\frac{D-1}{2}\right)} \int_0^\infty k^{D-2} dk \sum_{j \in \{u,d\}} \\
& \times \left(\ln \frac{1 + e^{-\beta(\sqrt{k^2 + (m_j + \sigma)^2} + \mu)}}{1 + e^{-\beta(\sqrt{k^2 + m_j^2} + \mu)}} + \ln \frac{1 + e^{-\beta(\sqrt{k^2 + (m_j + \sigma)^2} - \mu)}}{1 + e^{-\beta(\sqrt{k^2 + m_j^2} - \mu)}} \right). \quad (56)
\end{aligned}$$

The stable solution of the gap equation is obtained by observing the minimum of the effective potential. We numerically calculate it and show typical behaviors of the effective potential $V(\langle\sigma\rangle)$ and the dynamically generated quark mass $\langle\sigma\rangle$ in Fig.6. A first order transition takes place for $\mu = 300(\text{MeV})$. In the massless quark limit a phase transition occurs as is shown in Ref.[10]. Because of the explicit chiral symmetry breaking term, i.e. finite current quark mass, the phase transition becomes a cross over in Fig.6 [24, 25]. In Ref.[10] detailed behaviors of the dynamically generated mass and the phase structure are found for $m_u = m_d = 0$. Analytic expressions for some characteristic points are also presented there.

V. MESON MASSES AT FINITE T AND μ

Next we consider meson masses in a thermal equilibrium. The question of whether the Nambu-Goldstone modes of the chiral symmetry breaking are still massless or not at finite

T and μ is not trivial [26, 27, 28, 29, 30]. It is expected that the dispersion law is modified in the thermal equilibrium.

In the imaginary time formalism the self-energy for the pseudo-scalar channel, $\Pi_5^a(p^2)$ is modified as

$$\Pi_5^a(p_4, \mathbf{p}) = -4(g_\pi^0)^2 \frac{1}{\beta} \sum_n \int \frac{d^{D-1}\mathbf{k}}{(2\pi)^{D-1}} \text{tr}[i\gamma^5 \tau^a S(k)_{\beta\mu} i\gamma^5 \tau^a S(k-p)_{\beta\mu}]. \quad (57)$$

Performing the trace operation in Eq.(57), we obtain

$$\begin{aligned} \Pi_5^{1,2}(p_4, \mathbf{p}) = & 4N_c(g_\pi^0)^2 2^{D/2} \frac{1}{\beta} \sum_n \int \frac{d^{D-1}\mathbf{k}}{(2\pi)^{D-1}} \\ & \times \frac{(\omega_n - i\mu)(\omega_n - p_4 - i\mu) + \mathbf{k} \cdot (\mathbf{k} - \mathbf{p}) + (m_u + \langle\sigma\rangle)(m_d + \langle\sigma\rangle)}{[(\omega_n - i\mu)^2 + E_{1u}^2][(\omega_n - p_4 - i\mu)^2 + E_{2d}^2]} \\ & + (u \leftrightarrow d), \end{aligned} \quad (58)$$

and

$$\begin{aligned} \Pi_5^3(p_4, \mathbf{p}) = & 4N_c(g_\pi^0)^2 2^{D/2} \frac{1}{\beta} \sum_n \int \frac{d^{D-1}\mathbf{k}}{(2\pi)^{D-1}} \sum_{j \in \{u,d\}} \\ & \times \frac{(\omega_n - i\mu)(\omega_n - p_4 - i\mu) + \mathbf{k} \cdot (\mathbf{k} - \mathbf{p}) + (m_j + \langle\sigma\rangle)^2}{[(\omega_n - i\mu)^2 + E_{1k}^2][(\omega_n - p_4 - i\mu)^2 + E_{2k}^2]}, \end{aligned} \quad (59)$$

where

$$E_{1k}^2 = \mathbf{k}^2 + (m_j + \langle\sigma\rangle)^2, \quad E_{2k}^2 = (\mathbf{k} - \mathbf{p})^2 + (m_j + \langle\sigma\rangle)^2. \quad (60)$$

We observe the massless pole of the pion propagator at the massless quark limit, again. For $m_u = m_d = 0$ Eqs.(58) and (59) reduce to

$$\begin{aligned} \Pi_5^a(p_4, \mathbf{p}) = & 4N_c(g_\pi^0)^2 2^{D/2} \frac{1}{\beta} \sum_n \int \frac{d^{D-1}\mathbf{k}}{(2\pi)^{D-1}} \\ & \times \left[\frac{1}{[(\omega_n - i\mu)^2 + E_{1|m=0}]^2} + \frac{1}{[(\omega_n - p_4 - i\mu)^2 + E_{2|m=0}]^2} \right. \\ & \left. - \frac{p_4^2 + \mathbf{p}^2}{[(\omega_n - i\mu)^2 + E_{1|m=0}][(\omega_n - p_4 - i\mu)^2 + E_{2|m=0}]} \right]. \end{aligned} \quad (61)$$

To find the massless pole we put $p^2 = p_4^2 + \mathbf{p}^2 = 0$. Then the final line in Eq.(61) disappears. Since the pseudo-scalar field with the momentum p obeys the Bose-Einstein statistics, the fourth element p_4 is written as $p_4 = 2l\pi/\beta$ (l is an integer). We can simply change variables $\omega_n - p_4$ and $\mathbf{k} - \mathbf{p}$ in the third line in Eq.(61) to ω_n and \mathbf{k} respectively.

The pion self-energy (61) reduces to

$$\begin{aligned}\Pi_5^a(p^2 = 0) &= 8N_c(g_\pi^0)^2 2^{D/2} \frac{1}{\beta} \sum_n \int \frac{d^{D-1}\mathbf{k}}{(2\pi)^{D-1}} \frac{1}{(\omega_n - i\mu)^2 + \mathbf{k}^2 + \langle\sigma\rangle^2} \\ &= -\frac{4(g_\pi^0)^2}{\langle\sigma\rangle} \frac{1}{\beta} \sum_n \int \frac{d^{D-1}\mathbf{k}}{(2\pi)^{D-1}} \text{tr} S_{\beta\mu}(k).\end{aligned}\quad (62)$$

The pion mass at finite T and μ is found to be

$$\begin{aligned}Z_\pi^{-1} m_\pi^2(p^2 = 0) M_0^{D-4} &= \frac{1}{2g_\pi^0} - \frac{\Pi_5^a(p^2 = 0)}{4(g_\pi^0)^2} \\ &= \frac{1}{2g_\pi^0} + \frac{1}{\langle\sigma\rangle} \frac{1}{\beta} \sum_n \int \frac{d^{D-1}\mathbf{k}}{(2\pi)^{D-1}} \text{tr} S_{\beta\mu}(k).\end{aligned}\quad (63)$$

Substituting the gap equation (50) into Eq.(63), we find that the pion is also massless at finite T and μ . The pion is massless if the quark state is represented by a non-trivial solution of the gap equation. It is noteworthy that we do not use the Feynman parametrization. It is not applicable to calculate loops at finite T and μ .

Next we evaluate the contribution of the finite current quark mass. Here we consider the isospin symmetric limit for simplicity and set $m_u = m_d \equiv m$ again. In this case a pole of the pion propagator is given by

$$\begin{aligned}0 &= \frac{1}{2g_\pi^0} - \frac{\Pi_5^a(p_4, \mathbf{p})}{4(g_\pi^0)^2} \\ &= \frac{1}{2g_\pi^0} \left(1 - \frac{\langle\sigma\rangle}{\langle\sigma\rangle + m}\right) + N_c 2^{D/2} \frac{1}{\beta} \sum_n \int \frac{d^{D-1}\mathbf{k}}{(2\pi)^{D-1}} \\ &\quad \times \frac{p_4^2 + \mathbf{p}^2}{[(\omega_n - i\mu)^2 + E_1^2][(\omega_n - p_4 - i\mu)^2 + E_2^2]},\end{aligned}\quad (64)$$

where we have used the gap equation (50) in passing from the first line to the second and third one. Performing the summation in Eq.(64) [22], we get

$$\begin{aligned}0 &= \frac{1}{2g_\pi^0} \left(1 - \frac{\langle\sigma\rangle}{\langle\sigma\rangle + m}\right) - \frac{N_c 2^{D/2} (p_4^2 + \mathbf{p}^2)}{4} \int \frac{d^{D-1}\mathbf{k}}{(2\pi)^{D-1}} \frac{1}{E_1 E_2} \\ &\quad \times \left[\frac{1 - n_+(E_1) - n_-(E_2)}{ip_4 - E_1 - E_2} - \frac{n_-(E_1) - n_-(E_2)}{ip_4 + E_1 - E_2} \right. \\ &\quad \left. + \frac{n_+(E_1) - n_+(E_2)}{ip_4 - E_1 + E_2} - \frac{1 - n_-(E_1) - n_+(E_2)}{ip_4 + E_1 + E_2} \right],\end{aligned}\quad (65)$$

where

$$n_\pm(E) \equiv \frac{1}{e^{\beta(E \mp \mu)} + 1}.\quad (66)$$

To find the dispersion law in the Minkowski space we perform Wick rotation, $ip_4 \rightarrow p_0$. Thus the Eq.(65) reads

$$\begin{aligned}
0 = & \frac{1}{2g_\pi^0} \left(1 - \frac{\langle \sigma \rangle}{\langle \sigma \rangle + m} \right) + \frac{N_c 2^{D/2} (p_0^2 - \mathbf{p}^2)}{4} \int \frac{d^{D-1} \mathbf{k}}{(2\pi)^{D-1}} \frac{1}{E_1 E_2} \\
& \times \left[\frac{1 - n_+(E_1) - n_-(E_2)}{p_0 - E_1 - E_2} - \frac{n_-(E_1) - n_-(E_2)}{p_0 + E_1 - E_2} \right. \\
& \left. + \frac{n_+(E_1) - n_+(E_2)}{p_0 - E_1 + E_2} - \frac{1 - n_-(E_1) - n_+(E_2)}{p_0 + E_1 + E_2} \right]. \tag{67}
\end{aligned}$$

If we change variable \mathbf{k} to $\mathbf{p} - \mathbf{k}$ in Eq.(67), E_1 and E_2 are exchanged. Thus Eq.(67) simplifies to

$$\begin{aligned}
0 = & \frac{1}{2g_\pi^0} \left(1 - \frac{\langle \sigma \rangle}{\langle \sigma \rangle + m} \right) + \frac{N_c 2^{D/2} (p_0^2 - \mathbf{p}^2)}{2} \int \frac{d^{D-1} \mathbf{k}}{(2\pi)^{D-1}} \\
& \times \left[\left(\frac{1}{E_1} + \frac{1}{E_2} \right) \frac{1 - n_+(E_1) - n_-(E_1)}{p_0^2 - (E_1 + E_2)^2} \right. \\
& \left. + \left(\frac{1}{E_1} - \frac{1}{E_2} \right) \frac{-n_+(E_1) - n_-(E_1)}{p_0^2 - (E_1 - E_2)^2} \right]. \tag{68}
\end{aligned}$$

We divide the momentum integral in the radial and the angle parts,

$$\int d^{D-1} \mathbf{k} = \int_0^\infty k^{D-2} dk \int_0^\pi \sin^{D-3} \theta_1 d\theta_1 \cdots \int_0^\pi \sin \theta_{D-3} d\theta_{D-3} \int_0^{2\pi} d\theta_{D-2}. \tag{69}$$

We can choose the space coordinate in the direction $\mathbf{p} = (p, 0, 0, \dots)$, then $\mathbf{k} \cdot \mathbf{p} = kp \cos \theta_1$. The integrand in Eq.(67) depends only on k and θ_1 . The angle integrals with respect to $\theta_2 \cdots \theta_{D-2}$ give

$$\int_0^\pi \sin^{D-4} \theta_2 d\theta_2 \cdots \int_0^\pi \sin \theta_{D-3} d\theta_{D-3} \int_0^{2\pi} d\theta_{D-2} = \frac{2\pi^{D/2-1}}{\Gamma(D/2-1)}. \tag{70}$$

Thus the Eq.(68) reduces to

$$\begin{aligned}
0 = & \frac{1}{2g_\pi^0} \left(1 - \frac{\langle \sigma \rangle}{\langle \sigma \rangle + m} \right) \\
& + \frac{2N_c (p_0^2 - \mathbf{p}^2)}{(2\pi)^{D/2} \Gamma(D/2-1)} \int_0^\infty k^{D-2} dk \int_0^\pi \sin^{D-3} \theta_1 d\theta_1 \\
& \times \left[\left(\frac{1}{E_1} + \frac{1}{E_2} \right) \frac{1 - n_+(E_1) - n_-(E_1)}{p_0^2 - (E_1 + E_2)^2 - i\epsilon} \right. \\
& \left. + \left(\frac{1}{E_1} - \frac{1}{E_2} \right) \frac{-n_+(E_1) - n_-(E_1)}{p_0^2 - (E_1 - E_2)^2 - i\epsilon} \right]. \tag{71}
\end{aligned}$$

In the chiral limit $m \rightarrow 0$, the solution of this equation is $p_0^2 - \mathbf{p}^2 = 0$, as is shown before. A finite current quark mass changes the solution.

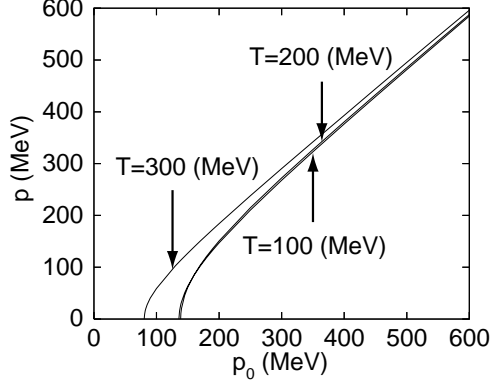
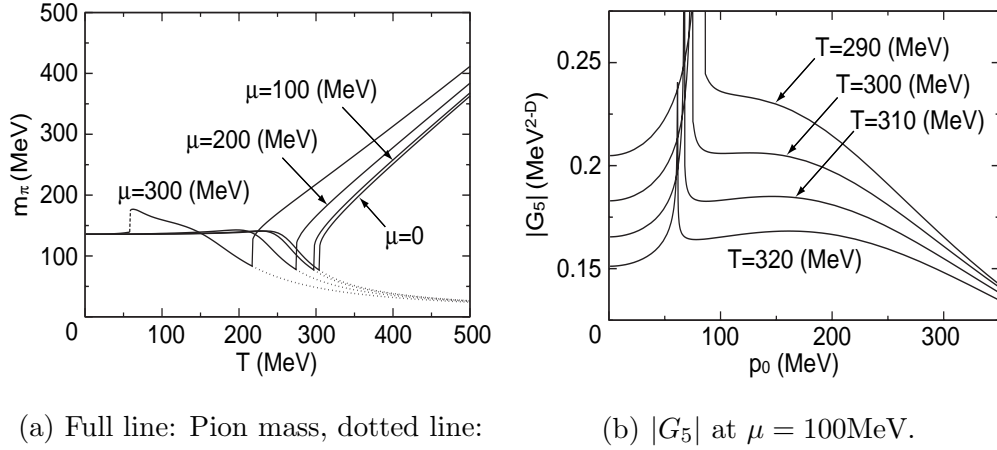


FIG. 7: Dispersion law for pion at $\mu = 0$ for $D = 2.4$ and $m_u = m_d = 5\text{MeV}$.



(a) Full line: Pion mass, dotted line:

$$-2(\langle\sigma\rangle + m).$$

(b) $|G_5|$ at $\mu = 100\text{MeV}$.

FIG. 8: Typical behaviors of the pion pole and $|G_5|$ at finite T and μ for $D = 2.4$ and $m_u = m_d = 5\text{MeV}$.

In the limit $\mu \rightarrow 0$ and $T \rightarrow 0$, the right hand side of Eq.(71) is a function of p^2 . To see if the finite T and μ modify this dispersion law we numerically solve Eq.(71). In the numerical analysis we put $D = 2.4$ and use the parameters determined in the subsection III.C. In Fig. 7 we plot the solutions on p_0, \mathbf{p} plane at finite T . The solutions are on hyperbolic curves as an usual $T = 0$ case. The value of p_0 on the curve at $\mathbf{p} = 0$ corresponds to the pion mass. The pion mass is obtained by solving Eq. (71) after rotating the contour by $-\pi/4$. A soft mode for the pion channel is found by observing an extremum of the absolute value of the propagator $|G_5|$. The pion mass decreases as T increases from 0 to the critical temperature T_c . A soft mode appears above T_c . We also draw the behaviors of $|G_5|$ near T_c in Fig. 8 (b).

The sharp peak structure is observed near $-2(\langle\sigma\rangle + m)$ for $T \gtrsim T_c$. In Fig. 8 (a) we see a gap at $T \simeq 60(\text{MeV})$ for $\mu = 300(\text{MeV})$. The gap comes from the one for $\langle\sigma\rangle$ in Fig. 6 (b).

For the scalar channel the self-energy, $\Pi_s(p_4, \mathbf{p})$ is given by

$$\Pi_s(p_4, \mathbf{p}) = -4(g_\pi^0)^2 \frac{1}{\beta} \sum_n \int \frac{d^{D-1}\mathbf{k}}{(2\pi)^{D-1}} \text{tr}[S(k)_{\beta\mu} S(k-p)_{\beta\mu}]. \quad (72)$$

We perform the trace operation and get

$$\begin{aligned} \Pi_s(p_4, \mathbf{p}) = & 4N_c(g_\pi^0)^2 2^{D/2} \frac{1}{\beta} \sum_n \int \frac{d^{D-1}\mathbf{k}}{(2\pi)^{D-1}} \sum_{j \in \{u,d\}} \\ & \times \frac{(\omega_n - i\mu)(\omega_n - p_4 - i\mu) + \mathbf{k} \cdot (\mathbf{k} - \mathbf{p}) - (m_j + \langle\sigma\rangle)^2}{[(\omega_n - i\mu)^2 + E_{1k}^2][(\omega_n - p_4 - i\mu)^2 + E_{2k}^2]}. \end{aligned} \quad (73)$$

It has the following relationship with the self-energy for the pseudo-scalar channel,

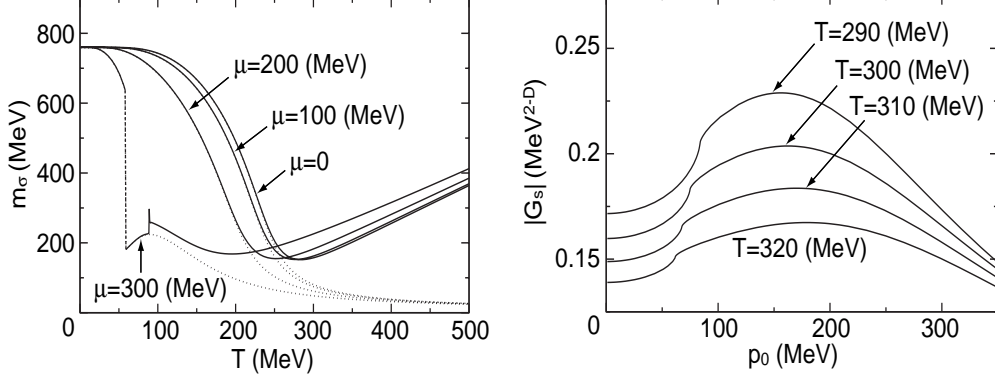
$$\begin{aligned} \Pi_s(p_4, \mathbf{p}) = & \Pi_5^3(p_4, \mathbf{p}) \\ & - \sum_{j \in \{u,d\}} 8(\langle\sigma\rangle + m_j)^2 N_c(g_\pi^0)^2 2^{D/2} \frac{1}{\beta} \sum_n \int \frac{d^{D-1}\mathbf{k}}{(2\pi)^{D-1}} \\ & \times \frac{1}{[(\omega_n - i\mu)^2 + E_{1k}^2][(\omega_n - p_4 - i\mu)^2 + E_{2k}^2]}. \end{aligned} \quad (74)$$

The difference between $\Pi_s(p_4, \mathbf{p})$ and $\Pi_5^3(p_4, \mathbf{p})$ disappears at the chiral limit $(\langle\sigma\rangle + m_j) \rightarrow 0$. If the chiral symmetry is restored, the scalar and the pseudo-scalar channel degenerate even for finite T and μ .

The two-point function for the scalar meson can be calculated similarly to Eq. (63) for the pion pole. After the summation over the Matsubara frequencies and the Wick rotation we obtain

$$\begin{aligned} G_s^{-1}(p_0, \mathbf{p}, \langle\sigma\rangle) = & \frac{1}{2g_\pi^0} \left(1 - \frac{\langle\sigma\rangle}{\langle\sigma\rangle + m} \right) \\ & + \frac{N_c 2^{D/2} (p_0^2 - \mathbf{p}^2 - 4(\langle\sigma\rangle + m)^2)}{4} \int \frac{d^{D-1}\mathbf{k}}{(2\pi)^{D-1}} \frac{1}{E_1 E_2} \\ & \times \left[\frac{1 - n_+(E_1) - n_-(E_2)}{p_0 - E_1 - E_2} - \frac{n_-(E_1) - n_-(E_2)}{p_0 + E_1 - E_2} \right. \\ & \left. + \frac{n_+(E_1) - n_+(E_2)}{p_0 - E_1 + E_2} - \frac{1 - n_-(E_1) - n_+(E_2)}{p_0 + E_1 + E_2} \right]. \end{aligned} \quad (75)$$

Adopting the mathematical trick used in Eq.(68) and integrating over the angle variables,



(a) Full line: sigma meson and soft mode masses, dotted line:

$$-2(\langle\sigma\rangle + m).$$

(b) $|G_s|$ at $\mu = 100\text{MeV}$.

FIG. 9: Typical behaviors of the sigma and pion pole at finite T and μ for $D = 2.4$ and $m_u = m_d = 5\text{MeV}$.

$\theta_2 \cdots \theta_{D-2}$, we get

$$\begin{aligned}
G_s^{-1}(p_0, \mathbf{p}, \langle\sigma\rangle) = & \frac{1}{2g_\pi^0} \left(1 - \frac{\langle\sigma\rangle}{\langle\sigma\rangle + m} \right) \\
& + \frac{2N_c(p_0^2 - \mathbf{p}^2 - 4(\langle\sigma\rangle + m)^2)}{(2\pi)^{D/2}\Gamma(D/2 - 1)} \int_0^\infty k^{D-2} dk \int_0^\pi \sin^{D-3} \theta_1 d\theta_1 \\
& \times \left[\left(\frac{1}{E_1} + \frac{1}{E_2} \right) \frac{1 - n_+(E_1) - n_-(E_1)}{p_0^2 - (E_1 + E_2)^2 - i\epsilon} \right. \\
& \left. + \left(\frac{1}{E_1} - \frac{1}{E_2} \right) \frac{-n_+(E_1) - n_-(E_1)}{p_0^2 - (E_1 - E_2)^2 - i\epsilon} \right]. \tag{76}
\end{aligned}$$

The sigma meson and soft mode masses are obtained by observing the extremum of $|G_s|$ after rotating the contour by $-\pi/4$. We draw the behaviors of the sigma meson mass and the soft mode in Fig. 9 (a). As temperature increases from 0 to T_c , the sigma meson mass decreases for $\mu \lesssim 200\text{MeV}$. The sigma meson mass turns into the soft mode at temperature above T_c . A gap at $\mu = 300\text{MeV}$ and $T \simeq 60\text{MeV}$ in Fig. 9 (a) is induced by the gap found in the $\langle\sigma\rangle$ behaviors shown in Fig. 6 (b). The other small gap appears at $T \simeq 100\text{MeV}$. It comes from the extremum of $\langle\sigma\rangle$ as is shown in Fig 6. (b). In Fig. 9 (a) we also draw $-2(\langle\sigma\rangle + m)$ where a naive threshold for $\bar{\psi}\psi$ state appears. The sigma channel above T_c we call the soft mode. In Fig. 9 (b) we show the extrema for $|G_s|$ which corresponds to the

soft mode.

VI. CONCLUSION

We studied characteristic features of the NJL model in the dimensional regularization. The dimensional regularization is applied to internal lines in loop integrals as usual. Since the model is not renormalizable, we can not take the four dimensional limit. Thus we assumed that the space-time dimensions appeared in the loop integrals is only a parameter of the effective theory to be fixed phenomenologically and evaluated some physical properties of the model in the space-time dimensions less than four. We take notice of that only the radiative corrections should be evaluated in the space-time dimensions less than four to keep the four-dimensional properties in the real world. We evaluate the classical parts in four dimensions.

In the NJL model we see that the approximate chiral symmetry is dynamically broken for a negative bare coupling. The constituent quark mass is also negative. After the renormalization, we can define the renormalized coupling constant. The dimensional regularization keeps most of symmetries. We have inspected the massless pole of the Nambu-Goldstone mode of the chiral symmetry breaking at the massless quark limit. Calculating the meson masses in the vacuum, we show that three pseudo-scalar modes have massless pole in the broken phase. It is the direct consequence of the Ward-Takahashi identity. In the dimensional regularization the Ward-Takahashi identity remains usual. We also see that the mass for the scalar mode is real and positive.

The coupling constant, the space-time dimensions and the renormalization scale can be fixed by the pion mass and its decay constant. The dimensions less than three, but more than two, are preferable to obtain the constituent quark mass about $300 \sim 400\text{MeV}$. The current quark mass has a non-negligible dependence on it. If we take the larger current quark mass, the constituent quark mass about 300MeV is realized for higher dimensions. However, a large chemical potential induces the first order phase transition for lower dimensions $2 \leq D \leq 3$ in the massless quark limit, as is expected in other approaches, such as the cut-off regularization [5, 31, 32], Schwinger-Dyson equation [33, 34] and the lattice QCD [35].

After we fix the parameters phenomenologically, we numerically calculate the constituent quark mass at finite T and μ . The first order transition is observed for $D = 2.4$ at $\mu =$

300MeV. We also evaluate the thermal influence on the meson masses in the leading order of $1/N$ expansion. We show the dispersion law for pion and the behaviors of meson masses. For lower temperature only a small influence is observed on the meson mass. It should be noted that boson loops have $O(T^2)$ contribution at finite temperature. A meson loop appears in the next to leading order of $1/N$ expansion. Though it is neglected in the present paper, the contribution from a meson loop may not be negligible at higher temperature.

Some problems remain. One should include the QED corrections to evaluate the neutral and the charged pion mass difference [36]. The color superconductivity is also interesting to consider in the extended NJL model by using the dimensional regularization [37].

Acknowledgments

The authors would like to thank M. Harada and T. Fujihara for useful discussions. T. I. is supported by the Ministry of Education, Science, Sports and Culture, Grant-in-Aid for Scientific Research (C), 18540276, 2007.

-
- [1] Y. Nambu and G. Jona-Lasinio, Phys. Rev. **122** 345 (1961), *ibid.* **124** 246 (1961).
 - [2] K. Higashijima, Prog. Theor. Phys. Suppl. **104** 1 (1991).
 - [3] B. Rosenstein, B. J. Warr and S. H. Park, Phys. Rept. **205** 59 (1991).
 - [4] U. Vogl, Prog. Part. Nucl. Phys. **27** 1995 (1991).
 - [5] T. Hatsuda and T. Kunihiro, Phys. Rept. **247** 221 (1994).
 - [6] H. Asami, N. Ishii, W. Bentz and K. Yazaki, Phys. Rev. C**51** 51 (1995).
 - [7] Y. Kikukawa and K. Yamawaki, Phys. Lett. B**234** 497 (1990).
 - [8] T. Muta, *Nagoya Spring School on Dynamical Symmetry Breaking* (ed. K. Yamawaki, World Scientific, 1992)
 - [9] H.-J. He, Y.-P. Kuang, Q. Wang and Y.-P. Yi, Phys. Rev. D**45** 4610 (1992).
 - [10] T. Inagaki, T. Kouno and T. Muta, Int. J. Mod. Phys. A**10** 2241 (1995).
 - [11] T. Inagaki, S. Mukaigawa and T. Muta, Phys. Rev. D**52** 4267 (1995).
 - [12] K. Ishikawa, T. Inagaki and T. Muta, Mod. Phys. Lett. A**11** 939 (1996).

- [13] T. Inagaki, Int. J. of Mod. Phys. A**11** 4561 (1996).
- [14] T. Inagaki, T. Muta and S. D. Odintsov, Prog. Theor. Phys. Suppl. **127** 93 (1997).
- [15] T. Inagaki and K. Ishikawa, Phys. Rev. D**56** 5097 (1997).
- [16] Yu. I. Shil'nov and V. V. Chitov, Phys. Atom. Nucl. **64** 2051 (2001).
- [17] S. Krewald and K. Nakayama, Ann. of Phys. **216** 201 (1992).
- [18] R. G. Jafarov and V. E. Rochev, Central Eur. J. Phys. **2** 367 (2004).
- [19] V. Dmitrasinovic, H.-J. Schulze, R. Tegen and R. H. Lemmer, Phys. Rev. D**52** 2855 (1995).
- [20] T. Inagaki, D. Kimura and T. Murata, Prog. Theor. Phys. **111** 371 (2004).
- [21] F. Sannino, and J. Schechter, Phys. Rev. D**52** 96 (1995), M. Harada, F. Sannino and J. Schechter, *ibid.* D**54** 1991 (1996).
- [22] M. Le Bellac, *Thermal Field Theory* (Cambridge University Press, 1996).
- [23] M. Gell-Mann, R. Oakes, B. Renner, Phys. Rev. **175** 2195 (1968).
- [24] T. Hatsuda and T. Kunihiro, Prog. Theor. Phys. **74** 765 (1985).
- [25] S. P. Klevansky, Rev. Mod. Phys. **64** 649 (1992).
- [26] H. Itoyama and A. H. Mueller, Nucl. Phys. B**218**, 349 (1983).
- [27] R. D. Pisarski and M. Tytgat, Phys. Rev. D**54** 2989 (1996).
- [28] D. Toublan, Phys. Rev. D**56** 5629 (1997).
- [29] N. Petropoulos, J. Phys. G**25** 225 (1999).
- [30] J. T. Lenaghan and D. H. Rischke, J. Phys. G**26** 431 (2000).
- [31] V. Bernard, U.-G. Meissner and I. Zahed, Phys. Rev. D**36** 819 (1987).
- [32] M. Asakawa and K. Yazaki, Nucl. Phys. A**504** 3478 (1989).
- [33] Y. Taniguchi and Y. Yoshida, Phys. Rev. D**55** 2283 (1997).
- [34] M. Harada and A. Shibata, Phys. Rev. D**59** 014010 (1999).
- [35] Z. Fodor and S. D. Katz, J. High Energy Phys. **03** 014 (2002).
- [36] T. Fujihara, T. Inagaki and D. Kimura, Prog. Theor. Phys. **117** 139 (2007).
- [37] T. Fujihara, T. Inagaki and D. Kimura, J. Phys. A**39** 6371 (2006).
- [38] We choose a space-time dimensions at $D = 2.4$ in Fig. 4 (b) and so on. The sigma meson mass for $D = 2.4$ seems to be a little bit larger than the real value, but general properties for the phase structure are similar to the other space-time dimensions.